AIAA 92-0409

Numerical and Experimental Analysis of Vortex Sheets Behind Lifting Surfaces

M. P. Warzecha
Boeing Commercial Airplane Group
Seattle, Washington

H. H. Horng
University of Michigan
Ann Arbor, Michigan

30th Aerospace Sciences
Meeting & **Exhibit**
January *6-9/1992/* Reno, NV

Numerical and Experimental Analysis of Vortex Sheets Behind Lifting Surfaces

M. P. Warzecha*
Boeing Commercial Airplane Group
Seattle, Washington

H. H. Horng**
University of Michigan
Ann Arbor, Michigan

Abstract

Vortex wake phenomena are crucial to modern aircraft design and operation. Based on an established theory, this study presents a computational model of the vortex sheet evolution behind lifting surfaces. Furthermore, experiments are conducted to assess the numerical results of this study. The computational model is applied to understand how alterations in planform geometry affect engine exhaust dispersion rate. Many other potential applications exist for this type of model.

Nomenclature

L'	sectional lift
U_∞	freestream velocity
b	wingspan
c	chord length
i, j	indices for point vortices
s	direction along vortex sheet
u_i	induced z-velocity in Trefftz plane
v_i	induced y-velocity in Trefftz plane
x	downstream direction
x/b	normalized downstream direction
y	direction normal to z in the Trefftz plane
z	spanwise direction
Γ'	local bound circulation
$\Gamma(s)$	filament strength distribution
δ	vortex sheet thickness
$\gamma(s)$	circulation density distribution
ρ	density
ω	vorticity

1. Introduction

Until recently, trailing vortex sheet research depended heavily on costly wind tunnel and flight tests. With the advent of digital computers, panel methods were used to model the 3-D vortex wakes behind aircraft. However, such 3-D panel methods require extensive computational effort. This investigation utilizes a 2-D vortex method to develop an accurate and inexpensive computational model of the trailing vortex sheet. This method was previously studied by Rosenhead [5] and Chorin and Bernard [1].

The understanding of airplane vortex wake phenomena is critical to commercial and military aviation. Powerful wake vortices generated by passenger airliners and transport aircraft are extremely hazardous, especially during take-off and landing. Air traffic must be spaced to avoid accidents. The direct consequence is that landing and takeoff rates are reduced below maximum airport capacity.

There are benefits from utilizing vortex wake phenomena. Military applications of vortex wakes include increasing airplane stealthiness through the wake mixing of hot engine exhaust. Studying vortex wakes may also help to develop methods of reducing induced drag.

In this investigation, the computational model represents the wake behind a lifting surface by a series of spanwise vortex filaments. Circulation strength distribution is dictated by the planform. A fourth-order Runge-Kutta integration scheme computes the wake evolution in incremental Trefftz-plane behind the lifting body. To avoid numerical instability, a smoothing parameter is used to desingularize the governing equations [4]. The YB-49 and the B-2 were chosen for this study because their close approximation to a lifting surface. Finally, experiments were performed to asses numerical results.

2. Theory

According to classical aerodynamics, an airfoil section can be modeled as a bound vortex with a sectional lift $L'(y)$ given:

$$L'(y) = \rho U \Gamma(y) \qquad (1)$$

Assuming the planform to be untwisted and composed of self-similar airfoils, the sectional lift is directly proportional to the airfoil chord length:

$$L'(y) \propto c(y) \qquad (2)$$

* Payload Design Engineer
Boeing Commercial Airplane Group
Member AIAA

** Graduate Student
The University of Michigan
Student Member AIAA

Since the sectional circulation is directly propomonal to lift, the local bound circulation strength is also propomonal to the chord length:

$$\Gamma(y) \propto c(y) \tag{3}$$

The change in bound circulation between adjacent sectional airfoils must form a vortex filament in the streamwise direction. The filament circulation density is qual to the difference in circulation between the adjacent differential wing sections, i.e.:

$$\gamma(y) \propto d\Gamma dy \tag{4}$$

Across the entire span of the lifting surface, this forms a vortex sheet composed of infinite filaments; therefore, the circulation density of each filament is propomonal to the local change in chord length. The individual filament circulation strength is given by:

$$\Gamma(y) = \gamma(y)ds \tag{5}$$

where ds is the width of an individual vortex filament. By substitution, the circulation strength of each filament is given by:

$$\Gamma(y) = \left(\frac{dc}{dy}\right)ds \tag{6}$$

For this investigation, the governing equation is the conservation of momentum expressed in terms of the vorticity field, Equation (7):

$$\left[\frac{\partial}{\partial t} + \mathbf{u}\cdot\nabla - \frac{1}{Re}\nabla^2\right]\omega(\mathbf{x},t) = \boldsymbol{\omega}\cdot\nabla\mathbf{u} \tag{7}$$

Since the compressibility effects are negligible in the trailing wake, this form of the momentum conservation essentially determines the evolution of the vortex sheet. Furthermore, two additional assumptions apply in this case. For typical aircraft applications, the diffusivity ($1/Re$) is small: therefore, the diffusion term can be neglected. As a consequence, there will be no physical elimination of vorticity due to mixing. The steady three-dimensional wake can be approximated with an unsteady two-dimensional flow in the Trefftz plane. This can be justified by the fact that the wake evolves faster in the Trefftz plane as compared to the downstrean direction. Hence, the stretching term, $\omega\cdot\nabla u$, disappears. Therefore, the following induced velocities are derived:

$$\frac{dx_i}{dt} = \sum_{i\neq j}\frac{\Gamma_j}{2\pi}\frac{-(y_i - y_j)}{(x_i - x_j)^2 + (y_i - y_j)^2 + \delta^2} \tag{8a}$$

$$\frac{dy_i}{dt} = \sum_{i\neq j}\frac{\Gamma_j}{2\pi}\frac{(x_i - x_j)}{(x_i - x_j)^2 + (y_i - y_j)^2 + \delta^2} \tag{8b}$$

To avoid numerical instability and singularity, the smoothing parameter, δ, is inserted [1&4]. Physically, δ represents the finite thickness of the vortex sheet

3. Numerical Model of the Vortex Sheet

As mentioned previously, a vortex sheet can be analytically modeled as an infinite series of vortex filaments, each with a circulation density determined by the local rate of change in chord length. Computationally, the vortex sheet is modeled as a finite series of filaments, each with a width of ds. With the stated assumptions, the computer performs the unsteady two-dimensional calculations in Trefftz planes behind the lifting body. All displacements are normalized by the wingspan. At each Trefftz plane, the induced velocities of all vortex filaments are calculated and summed using Equation (8). Using the forth-order Runge-Kutta integration scheme, each point is advanced to the next Trefftz plane. This marching procedure represents the sheet evolution in time.

As the wake calculation progresses, the spacing between individual vortex filaments increases; therefore, additional points are inserted to insure adequate filament resolution. If the displacement between adjacent filaments exceeds a predefined value, Newton's polynomial interpolation is utilized to approximate the shape of the vortex sheet. The circulation strengths of the inserted point and its neighboring points are adjusted accordingly. Conversely, high concentration of filaments occur in specific areas of the vortex sheet. Extra computation docs not justify the limited sheet description gained from excessively high filament concentration Future program modifications may include a point-ranoval scheme. Before implementing a full scale analysis, three test cases involving point-vortex pairs were conducted to insure program integrity,

4. Numerical Results

For this investigation, two aircraft are chosen for full scale analysis of vortex sheet evolution, the Northrop YB-49 and the Northrop B-2 Stealth Bomber. The aircraft are flying wings that can be represented as lifting surfaces fining the scope of this study.

4.1 YB-49 Planform

The YB49 provides a simple delta-wing planform[2] with a known vortex sheet evolution. hence it is useful in verifying the full scale implementation of the computational model. The vortex sheet of the YB-49 can also be used as a comparison for the B-2. The vertical stabilizers and the small fuselage section arc ignored due to their minimal contribution to the vortex sheet. The planform of the YB-49 and the corresponding circulation density distribution are shown in Figure 1. In the this planform, it is worthy to note the infinite circulation density values at the wing tip caused by the chord-length discontinuities.

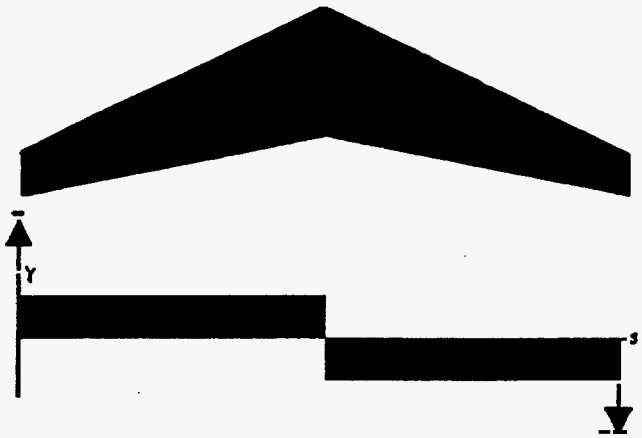

Figure 1 YB-49 planform and circulation density distribution

As expected, the simple delta-wing planform of the YB-49 produces a pair of counter-rotating vortices. Figure 2 shows the vortex sheet evolution of the YB49 at various normalized downstream locations.

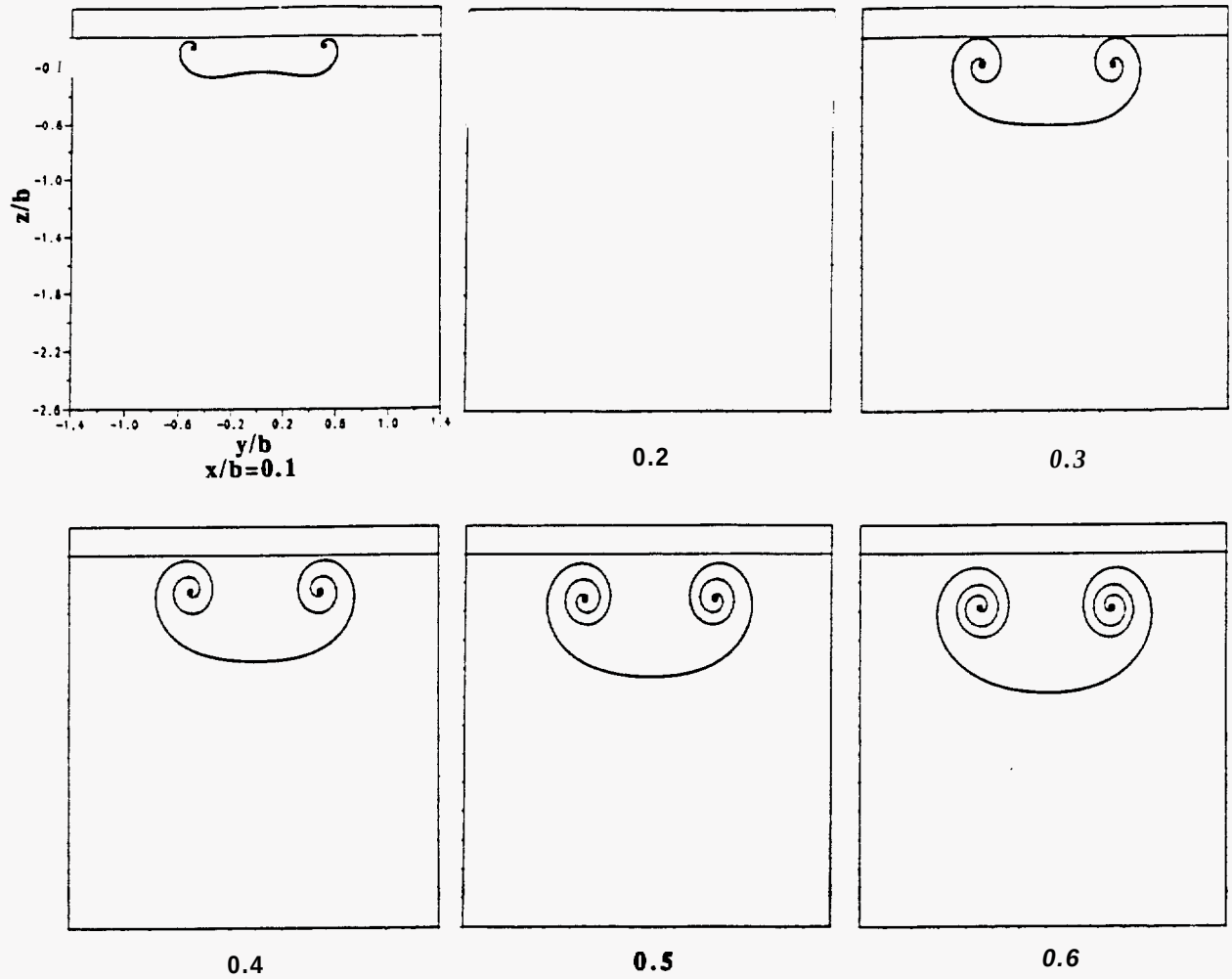

Figure 2 YB-49 vortex sheet evolution

4.2 B-2 Planform

The B-2 has a more interesting planform[6]. Although there are no chord-length discontinuities in this planform, the "saw-tooth-like" trailing edge provides an unique, yet somewhat regular, circulation density distribution shown in Figure 3.

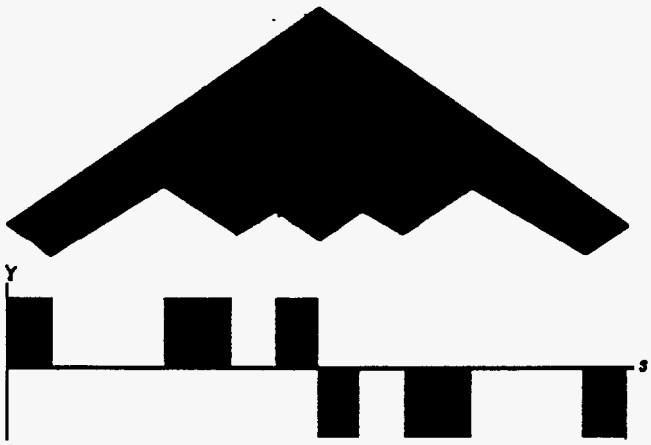

Figure 3 B-2 planform and circulation density distribution

The vortex sheet evolution of the B-2 does not resemble a conventional roll-up. The unique circulation density distribution creates a vortex sheet consisting mainly of *two* counter-rotating vortex pairs (*Figure* 4). For a purpose explained later, the points corresponding to the engine exhaust are marked with circles. Note that at a significant downstream distance the vortex sheet evolves into a counter-rotating vortex pair.

4.3 B-2 Modifications

This vortex tracking technique is applicable in many areas of aircraft design and fluid dynamics. For example, this technique may be used to produce a first-order approximation of exhaust detectability and to provide insight into planform modifications to reduce the detectability. As part of the investigation, this example concentrates on how the vortex sheet evolution disperses the engine exhaust and improves dispersion rate. One must keep in mind that other design features also contribute to the dispersion of exhaust gas.

The detectability approximation includes the following assumptions. The detectability of a passive *scalar* in the trailing *wake,* e.g. the thermal energy introduced by the exhaust, is inversely proportional to the rate *at* which the engine arc-length increases. "Engine arc-length" is defined as the length of the arc formed by the exhaust points along the s-direction *at* any normalized downstream locations. Throughout the vortex sheet evolution, the points corresponding to engine exhaust *arc* individually marked by a circle. Furthermore, to avoid difficulties in

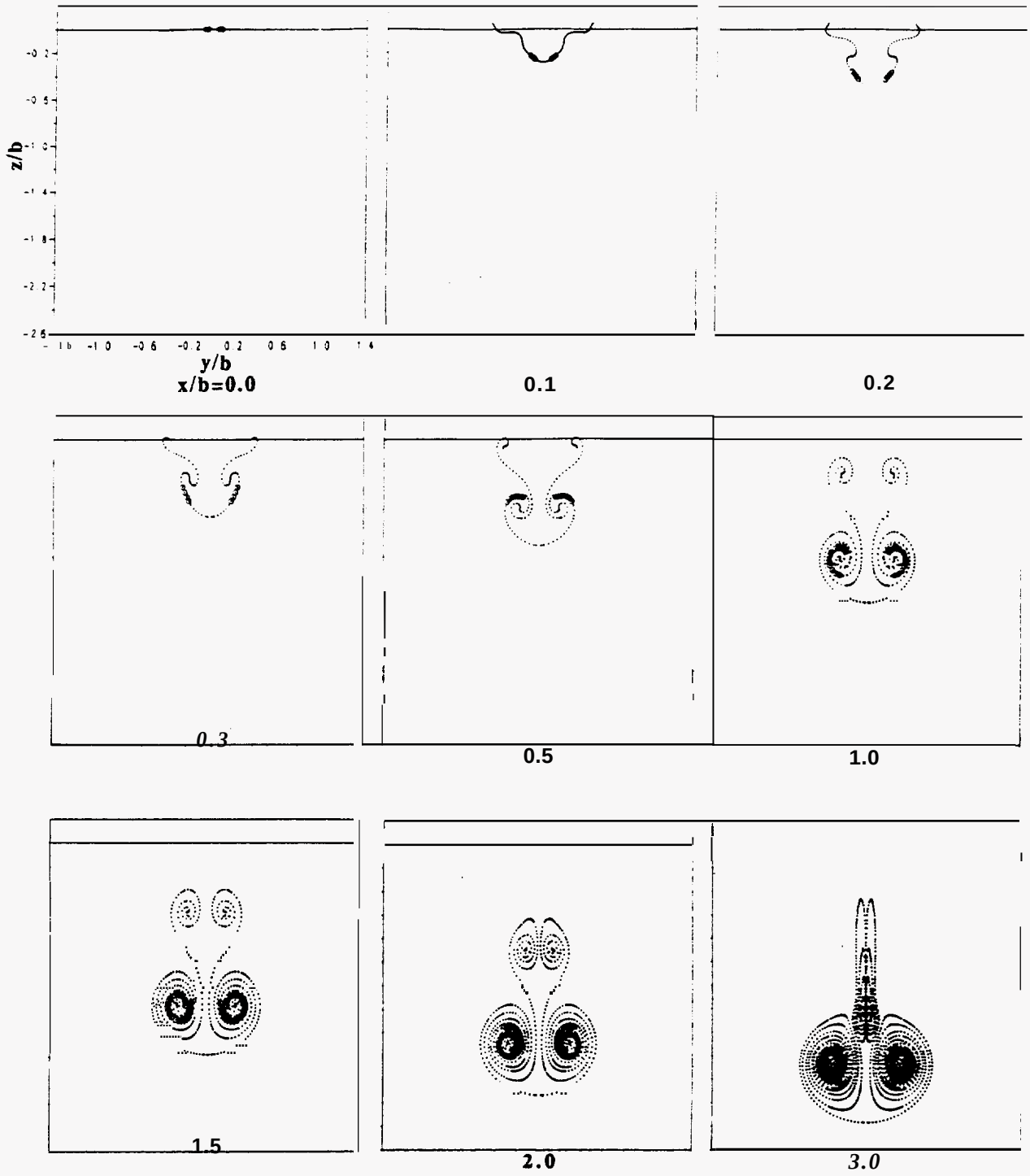

Figure 4 B-2 vortex sheet evolution

modeling the complex mixing process between exhaust and ambient air, it is assumed that the exhaust velocity equals the freestream velocity.

Several planform deviations from the *original* B-2 are studied in an attempt to understand how changes in the circulation density distribution, $\gamma(s)$, affects the dispersion rate. To reduce the impact on *other* design considerations, minimal changes are made in each planform modification.

The most important insight obtained is that drastic changes in $\gamma(s)$ the exhaust nozzles are most effective in increasing $\rho\sim$ dispersion rate. The modified planform with the greatest increase in dispersion rate, designated as the YB-2EF, is shown in Figure 5 with its circulation density distribution.

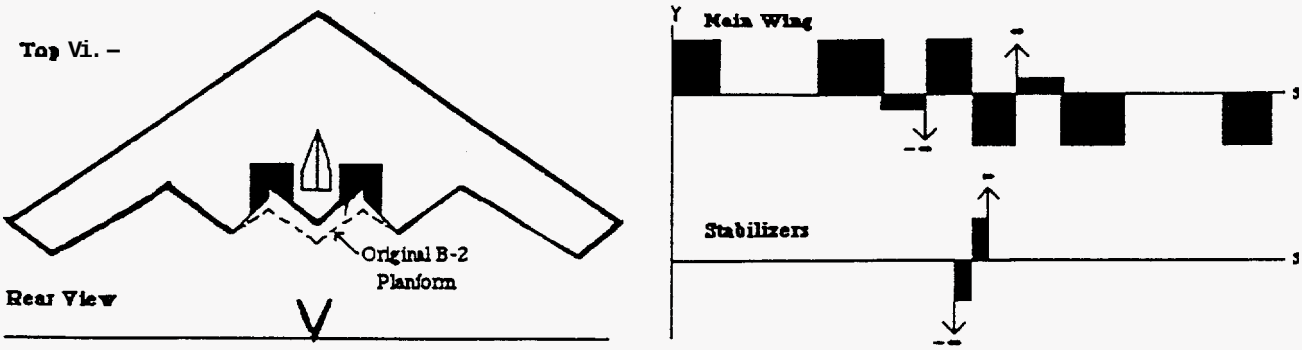

Figure 5 YB-2EF planform and circulation density distribution

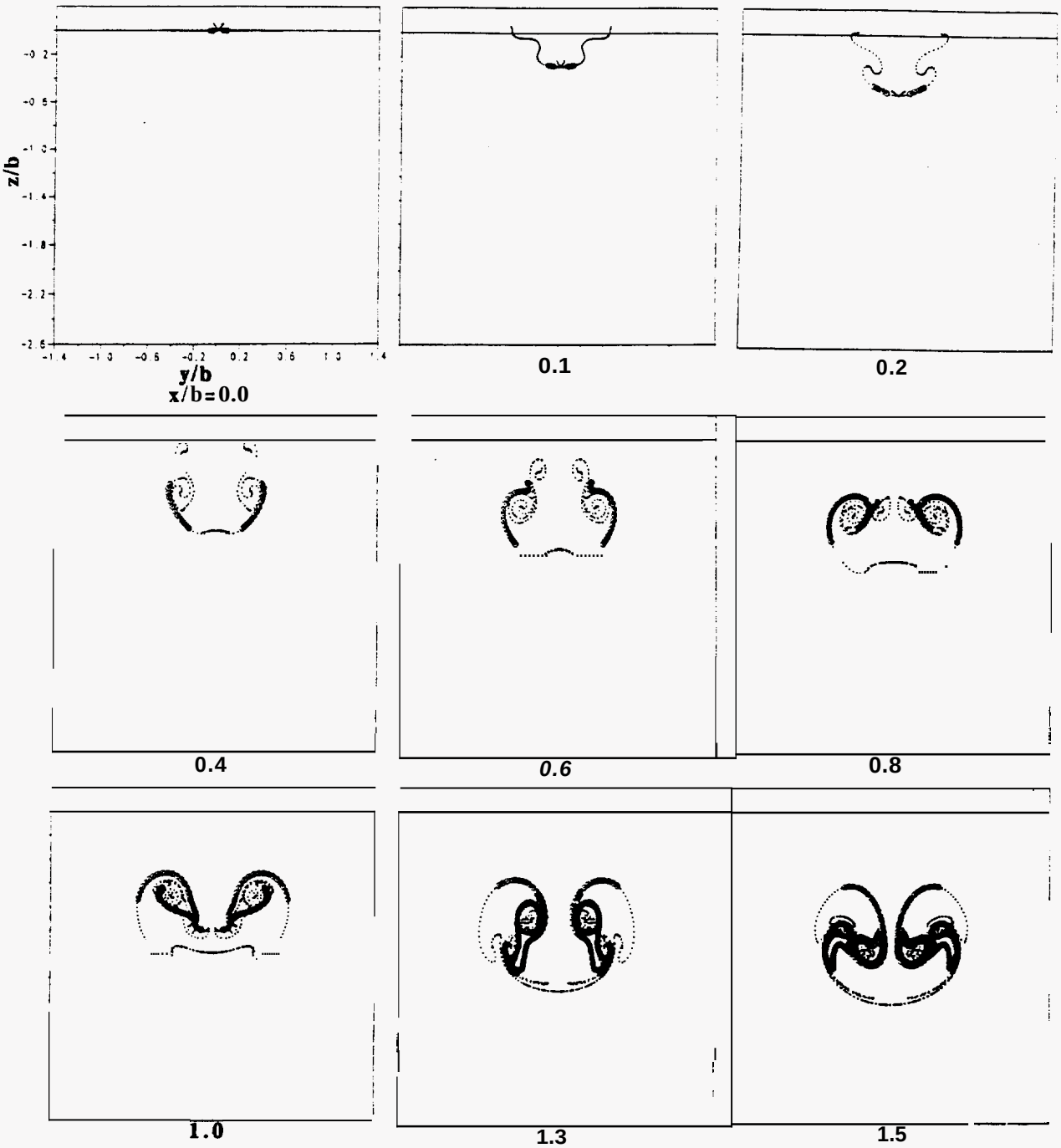

Figure 6 YB-2EF vortex sheet evolution

The V-tail is placed along the centerline with a 70° included angle similar to the F-117. The included angle prevents the tail from acting as a corner radar reflector[3]. Unlike the rest of the planform, the V-tail produces negative lift which results in a negative $\gamma(s)$ for the left tail and a positive value for the right. The tips of the V-tail provide theoretically infinite circulation density values due to the discontinuities in the chord length rate of change.

As compared to the B-2. the circulation density for the center-most section of the YB-2EF is unchanged. By changing the trailing edge slope of the next outboard sections, dc/dy becomes negative for the left outboard section and positive for the right outboard section. Although the circulation density value remains the same for the center-most section, the actual chord lengths are shortened to introduce mother set of theoretically infinite circulation density values at the centers of the exhaust nozzles. This modification plays an important role in increasing the dispersion rate. Figure 6 demonstrates the vortex sheet evolution of the YB-2EF, and Figure 7 shows a direct comparison of the engine arc-length growth rate between the YB-2EF and the B-2. Although the modifications may have reduced the thermal detectability, vulnerability of aircraft detection by other means and manufacturing difficulties may have been simultaneously increased.

5. Experimental Assessment

The experimental portion of this investigation was conducted at the University of Michigan Aerospace Engineering Department towing tank facility. The experimental results assess the accuracy and validity of the computational model.

The experiment consists of towing a scaled B-2 model in a water tank. The model is mounted at approximately 12° angle of attack and supported at the centerline. As the model travels downstream, gravity-fed laser fluorescent dye emerges from a milled opening on the pressure side of the model. A neon-argon laser beam, oscillating at approximately 180 Hz, produces a laser sheet normal to the freestream, analogous to the numerical Trefftz-plane. The laser sheet excites the dye molecules and reveals the two-dimensional structure of the vortex sheet, enabling a *camera* to photograph the evolution

Figure 8 shows the various frames of the experimental vortex sheet evolution. Two separate mals are shown, Frames (a) through (d) and Frames (e) through (h). In (a) through (d), the initial vortex sheet development is clearly shown. In this trial run. the dye passage was partially blocked causing the missing section in the right half of the vortex sheet.

Although the B-2 is the only planform tested in the towing tank, the results were sufficient to assess the validity of the numerical model. The general shape of the vortex sheet at various downstream locations is in close agreement with the numerical output As demonstrated by the experiment, the upper vortex pair collapses and mixes more rapidly with the lower vortex pair. This mixing phenomenon would have been obtained numerically if the computations were performed to a farther x/b. In addition, Frames (e) and (f) show that the vortex sheet evolves into a pair of counter-rotating vortices, as stated earlier.

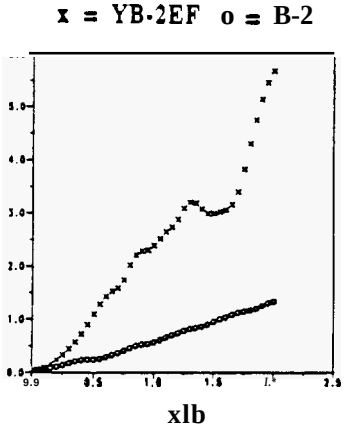

Figure 7 (a) Comparison of engine arc-length growth rate between YB-2EF and B-2

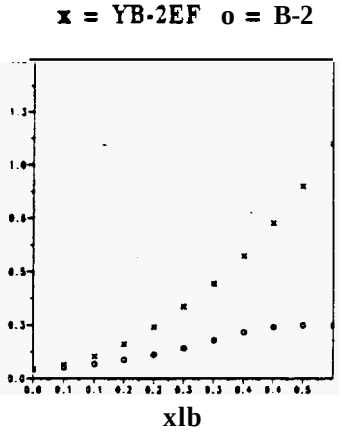

Figure 7 (b) Comparison of the early stages

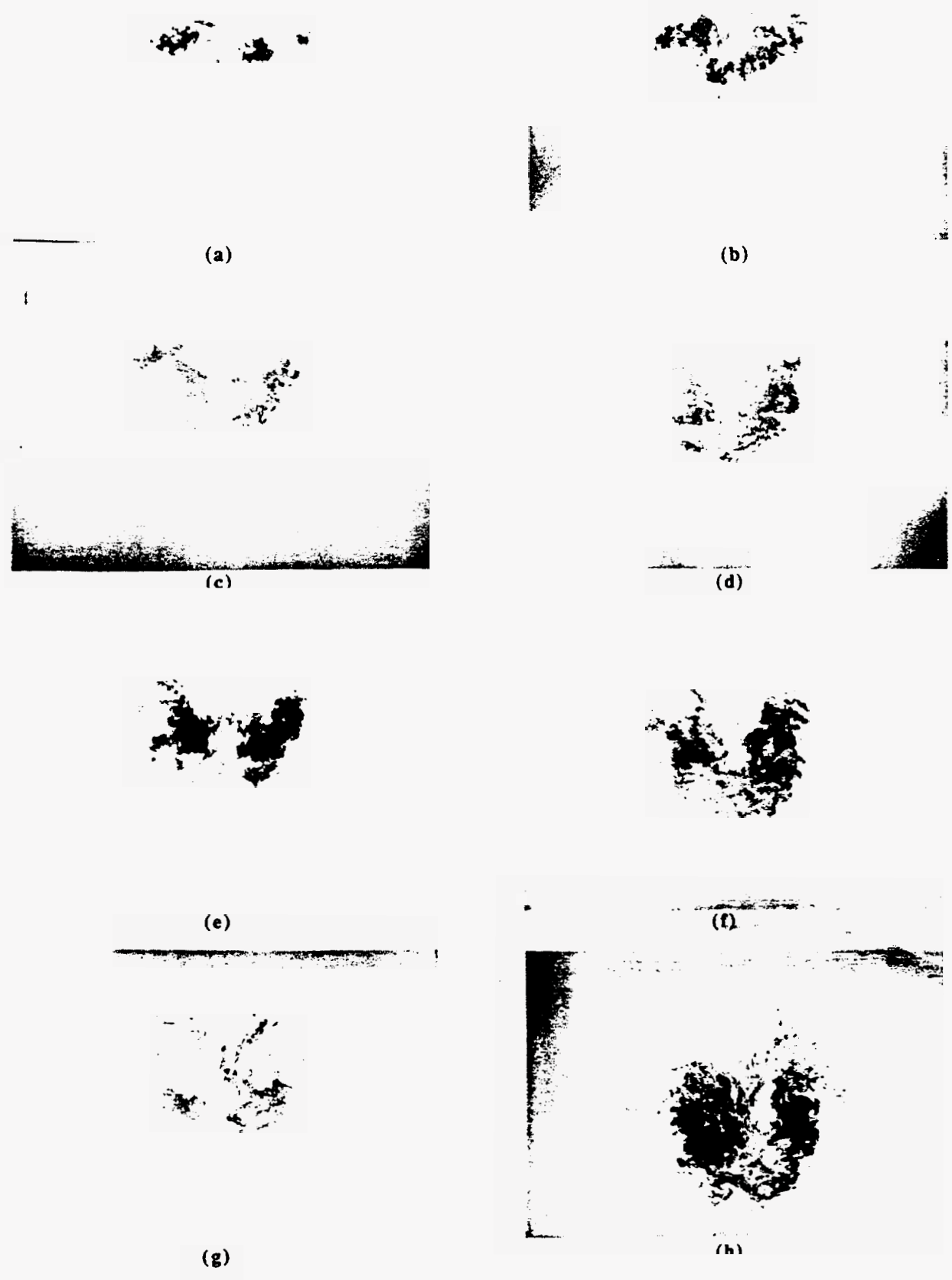

Figure 8 B-2 experimental vortex sheet evolution

6. Conclusions

This study has developed a simple numerical model of lifting body vortex wakes. Two aircraft are used for full scale implementation, the YB-49 and the B-2. The aircraft are chosen for their close resemblance to lifting bodies. Experimental data demonstrated that the computational model satisfactorily simulates the vortex sheet evolution.

This investigation utilizes the computational model to obtain an approximation of the exhaust dispersion phenomenon. Modifications are made to the B-2 planform to understand how the exhaust dispersion rate is affected by planform geometry. One major observation is made from the modifications. Discontinuities placed near the exhaust nozzles are significant factors in increasing the dispersion rate. An important conclusion from this example is that small modifications in planform geometry can considerably alter the vortex wake evolution and the corresponding dispersion rate.

7. Future Applications

Before applying the vortex tracking technique to more complicated problems, other topics must be addressed in order to make this a more complete tool. The topics include: presence and effects of the fuselage and empennage on the vortex sheet, ground effect, and three-dimensional mixing of the exhaust air.

To more accurately model an airplane, the presence of the empennage and the fuselage must also be considered. The empennage control surfaces can be modeled with the same vortex tracking technique; however, fuselage effects require a more complex technique. To simulate take-off and landing conditions, the ground effect can be modeled with the method of imaging. In addition, cross-wind effect can be simulated by assigning a pre-specified induced velocity on the filaments. In reality, the aircraft exhaust velocity does not equal the freestream velocity. Therefore, the three-dimensional mixing effects of the exhaust must be considered to more accurately model dispersion phenomenon.

In addition to the example application investigated, this vortex tracking technique is also useful in other areas of fluid dynamics and aircraft design. Further understanding of the trailing wake phenomenon can assist in optimizing the airport take-off and landing rates. Other military applications exist for this technique. In addition to reducing the aircraft thermal detectability. this technique may also be applied to reduce the trailing wake disturbance introduced. A major concern in submarine warfare is the detection of free surface signature produced by the control surfaces. This technique may aid in reducing the free surface signature.

References

1. Chorin, A.J. and Bernard, P.S., "Discretization of a Vortex Sheet, with an Example of Roll-Up," *J. Computational Physics*, 1973, Vol. 13, pp. 423-429.
2. Coleman, T., Jack Northrop and the Flying Wing. New York Paragon House, 1988.
3. Dornheim, MA., "USAF Display of F-117A Reveals New Derails of Stealth Aircraft," *Aviation Week and Space Technology* April 30, 1990: 31
4. Krasny, R., "Desingularization of Periodic Vortex Sheet Roll-Up," *J. Computational Physics*, 1986, Vol. 65, pp. 292-313.
5. Rosenhead, L., "The Formation of Vorticies From a Surface of Discontinuity," *Proc. Royal Society of London*, 1931, Vol. 134. p. 170.
6. Sweetman, B. Stealth Bomber. pp. 91-102. Osceola: Motorbooks Int, 1989.

Acknowledgments

This project was conducted under the guidance of Professor W.J.A. Dahm, the University of Michigan Department of Aerospace Engineering.